JOURNAL OF SOLID STATE CHEMISTRY **133,** 132–139 (1997)
ARTICLE NO. SC977331

Interband Critical Points of Some Icosahedral Boron-Rich Solids

H. Werheit,*,[1] C. Janowitz,† R. Schmechel,* T. Tanaka,‡ and Y. Ishizawa‡

** Solid State Physics Laboratory, Gerhard Mercator University Duisburg, D-47048 Duisburg, Germany; † Institute of Physics, Humboldt University Berlin, D-10115 Berlin, Germany; and ‡ National Institute for Research in Inorganic Materials, Tsukuba 305, Japan*

Received January 30, 1997; accepted February 12, 1997

The complex dielectric functions of β-rhombohedral boron, of boron carbide with compositions between $B_{4.23}C$ and $B_{10.37}C$ and YB_{66}, were measured between about 2.5 and 9.5 eV. Similarities of the electronic structures probably due to the icosahedra are indicated by obvious qualitative similarities of the spectra. Numerous critical points have been determined and confirm the dense sequence of energy bands. For β-rhombohedral boron the critical points are compatible with the combined density of states maxima derived from cluster calculations by K. Shirai and H. Nakamatsu (1994, *in* "Proc. 11th Int. Symp. Boron, Borides and Related Comp, Tsukuba, 1993," JJAP Series 10, p. 70). Otherwise no satisfactory correlation with theoretical band structure calculations is possible. In the case of boron carbide the critical points are the same within the whole homogeneity range, while the values of the dielectric function at higher energies indicate composition-dependent densities of states, which are correlated with the density of B_{12} icosahedra. © 1997 Academic Press

INTRODUCTION

B_{12} icosahedra are the common features of the different structure groups of icosahedral boron-rich solids. In the crystalline modifications these icosahedra are periodically arranged and their orbitals are essentially responsible for the electronic structures, which are accordingly expected to be related to one another as well. In consequence of a static Jahn–Teller effect the icosahedra are distorted, the I_h symmetry of the regular icosahedron is often reduced to D_{3d}, and the degeneracy of electronic states is accordingly lifted. For example, this explains that the boron-rich solids are semiconductors despite the odd electron number of the boron atom (1).

Apart from some modestly resolved density of states distributions of β-rhombohedral boron determined by XPS, SXS, Bremsstrahlung isochromate, and photoelectric yield investigations (see (2) and references therein) the experimentally determined interband transitions have been largely restricted to the absorption edges and yield the band gaps of these semiconductors. Largely reliable quantitative results are available, e.g., for β-rhombohedral boron (3), boron carbide (4), $B_{12}P_2$ (5,6) YB_{66} (7), some orthorhombic borides (8), and some α-AlB_{12} and γ-AlB_{12} representatives (9). Theoretical band structure calculation by different authors (10–15) are not consistent with one another, and in particular the calculated band gaps are usually by far too large compared with the experimental results indicating systematic errors in the theoretical calculations.

In this paper critical points in the interband transition range of some boron-rich solids are derived from the dielectric functions determined by spectroscopic ellipsometry between about 2.5 and 9.5 eV.

SAMPLES AND PREPARATION

β-Rhombohedral boron (structure formula $(B_{12})_4(B_{28})_2B$) was available in the form of high-purity single crystals (Wacker, Munich). Apart from carbon (about 60 ppm) the claimed purity is 99.9999%. Technical boron carbide (structure formula $(B_{12})_X(B_{11}C)_{1-X}$ $(CBC)_Y(CBB)_Z$ with $Y + Z \leq 1$) of different chemical composition partly prepared by melting and partly by hot pressing was provided by ESK, Kempten, and by H. C. Starck, Laufenburg. The investigated compositions vary from $B_{4.3}C$ at the carbon-rich limit of the homogeneity range to $B_{10.37}C$, which is close to the boron-rich limit assumed to be at about $B_{11}C$ or $B_{12}C$. At the carbon-rich limit of the homogeneity range additionally a 92% isotope-enriched $B_{4.3}C$ was investigated (for material details see (16)). The used single crystalline YB_{66} (structure formula $(B_{12}(B_{12})_{12}B_{48})_8Y_{\approx 24}$) was prepared at NIRIM, Tsukuba (see (17)). Apart from YB_{66}, whose cleaved surface was not further treated, the sample surfaces were prepared by mechanical grinding with diamond powders of gradually reduced grain size (finest grade 1 μm) and in the case of β-rhombohedral boron additionally chemically etched in a solution of $K_3[Fe(CN)_6]$, KOH in H_2O (18), which does not attack boron carbide. Some of the boron carbide samples, in particular those which were obtained by hot pressing, are not completely dense. This leads in some cases to

---

[1] To whom correspondence should be addressed.

0022-4596/97 $25.00

a remarkable loss of the reflected light by scattering, which affects the absolute values of the dielectric function.

EXPERIMENTAL

The measurements were performed with a VUV ellipsometer, described previously (14), utilizing linearly polarized radiation at the 2m-Seya Namioka beamline from the BESSY storage ring at Berlin. The high degree of linear polarization at energies $\hbar\omega > 4\,\mathrm{eV}$ enables measurements without entrance polarizer. At lower energies due to an increasing contribution of circular polarized radiation especially, the absolute ε_1 values are expected to be too low. The energetic positions of the structures remain mostly unaffected. The angle of incidence used was 67.5°. The entire ellipsometer can be rotated around the axis of the incoming light to change the angle between the plane of incidence and the plane of polarization. The dielectric functions of all samples were determined after transfer under air pressure. Effects due to oxygen overlayers on the samples were not accounted for, so that by applying the isotropic two-phase model for data processing only the so-called pseudo-dielectric function was obtained.

RESULTS

In Fig. 1 the real and imaginary parts of the dielectric functions of β-rhombohedral boron, boron carbide (composition $B_{4.3}C$), and YB_{66} belonging to different structure groups are plotted for comparison. Figure 2 shows a selection of spectra of boron carbides with different chemical compositions and of isotope-enriched $^{10}B_{4.3}C$.

Type, energy, and lifetime broadening of a van Hove singularity can be obtained by analyzing the derivative spectra of the real and imaginary parts of the dielectric functions (see (20)). The energy of the van Hove singularities is close to the minima of the second derivatives. To estimate the types, the first derivatives must be taken into account as well, and for a reliable determination of all parameters a complete fitting of all derivative spectra would be needed, in particular for close sequences of critical points like in the boron-rich solids. As examples, in Figs. 3 to 5 the numerically calculated second-derivative spectra of the real and imaginary parts of the experimentally determined dielectric functions of β-rhombohedral boron, isotope-enriched $^{10}B_{4.3}C$ and YB_{66} are shown. The spectrum of isotope-enriched boron carbide is chosen because the van Hove singularities are distinctly more pronounced than in the case of boron carbides with natural isotope distribution (19.8% ^{10}B, 80.2% ^{11}B).

The energetical positions of the minima of the second derivatives of the dielectric functions, the estimated critical point energies, and the assumed types of the van Hove singularities are listed in Tables 1 to 3 for β-rhombohedral boron, for the boron carbides, and for YB_{66} respectively. The estimated types of critical points are tentative only; they are estimated from the qualitative behavior of the first derivatives of ε_1 and ε_2 in the surrounding of the critical points.

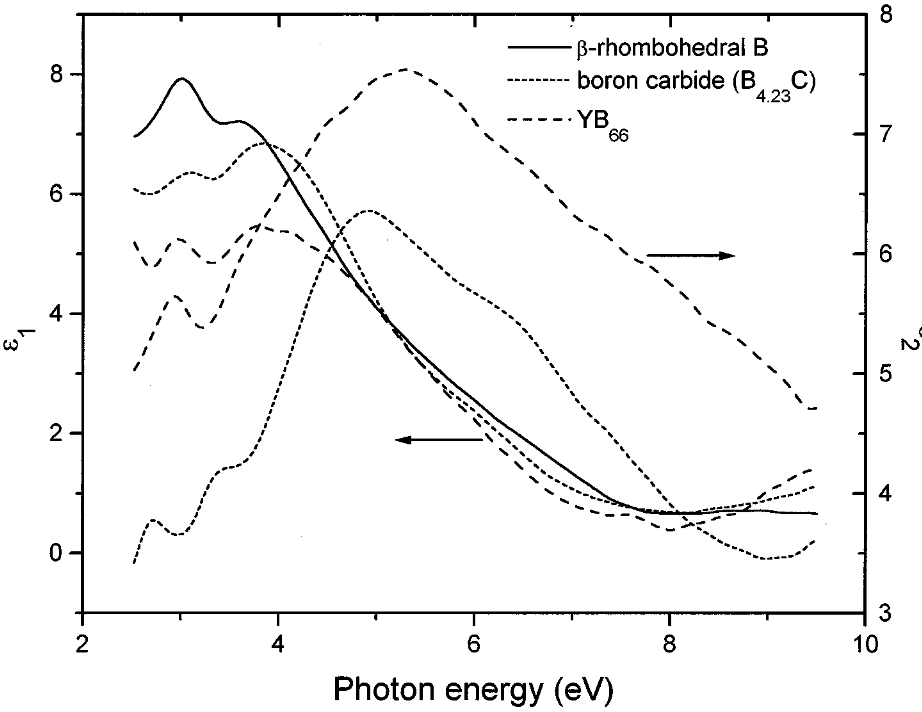

FIG. 1. Real and imaginary part of the dielectric functions of β-rhombohedral boron, boron carbide ($B_{4.3}C$), and YB_{68}.

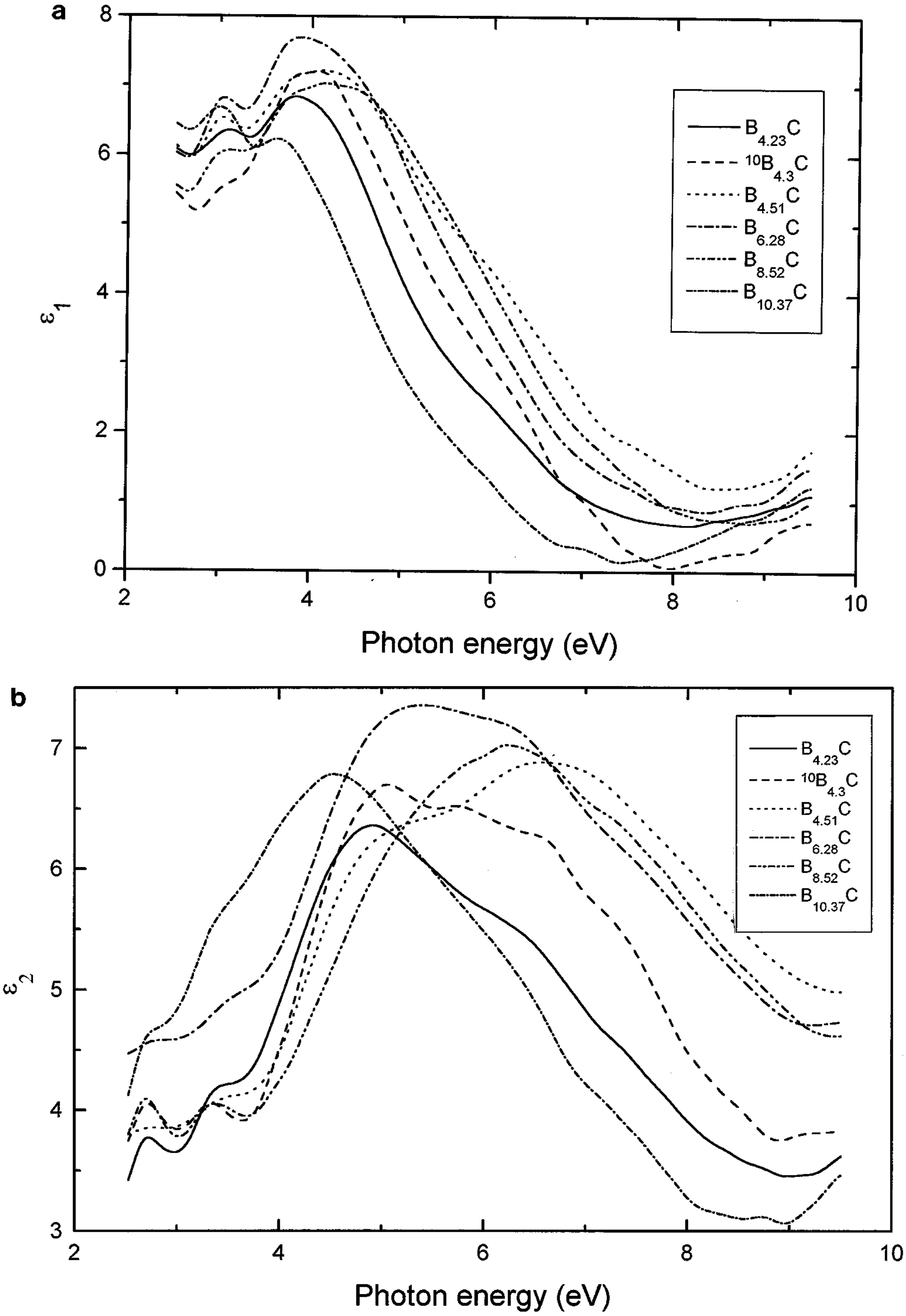

FIG. 2. Real (a) and imaginary part (b) of the dielectric functions of boron carbides with different chemical compositions ($B_{4.23}C$, $B_{4.51}C$, $B_{6.28}C$, $B_{8.52}C$, $B_{10.37}C$) and $^{10}B_{4.3}C$ (92% isotope-enriched).

DISCUSSION

The spectra of the dielectric functions of all the boron-rich solids investigated in this paper are qualitatively similar. They exhibit comparably narrow structures at roughly the same lower energies and a broad less-resolved peak at higher energies. This qualitative agreement confirms the expected relationship of the electronic structures of the

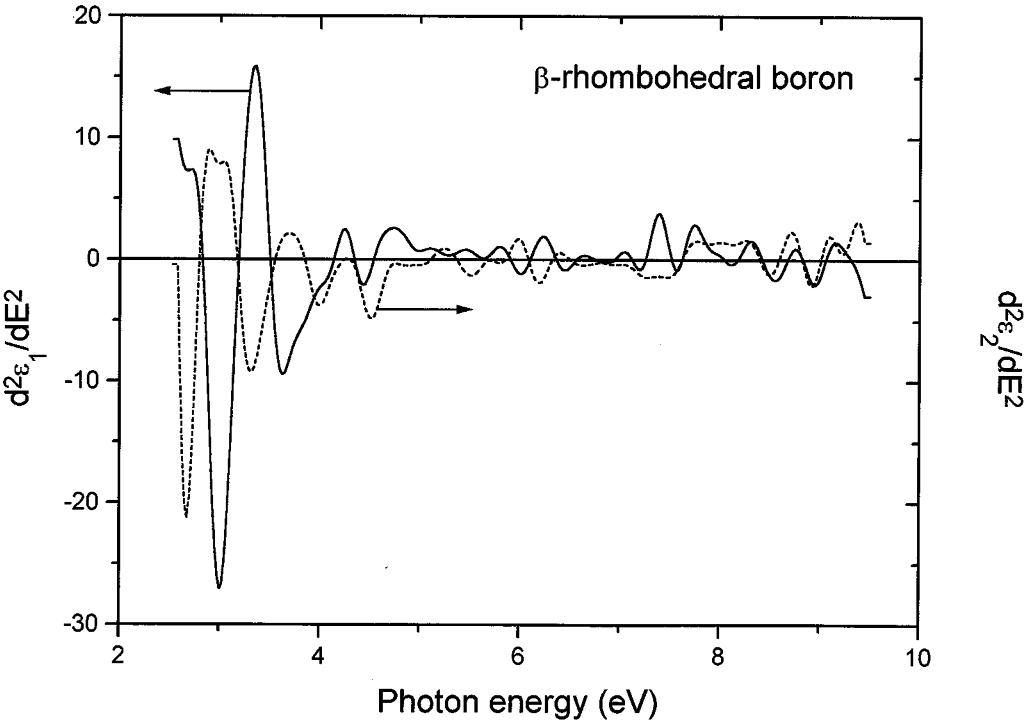

FIG. 3. Second derivatives of the real and imaginary parts of the dielectric function of β-rhombohedral boron.

boron-rich solids due to the icosahedra as common structural elements and accordingly to a considerable degree independent of the specific structures in the different structure groups which they belong to.

The theoretical band structure calculations of the different authors for the icosahedral boron-rich solids agree only in so far to one another as they establish close sequences of branches in the valence and in the conduction bands. This

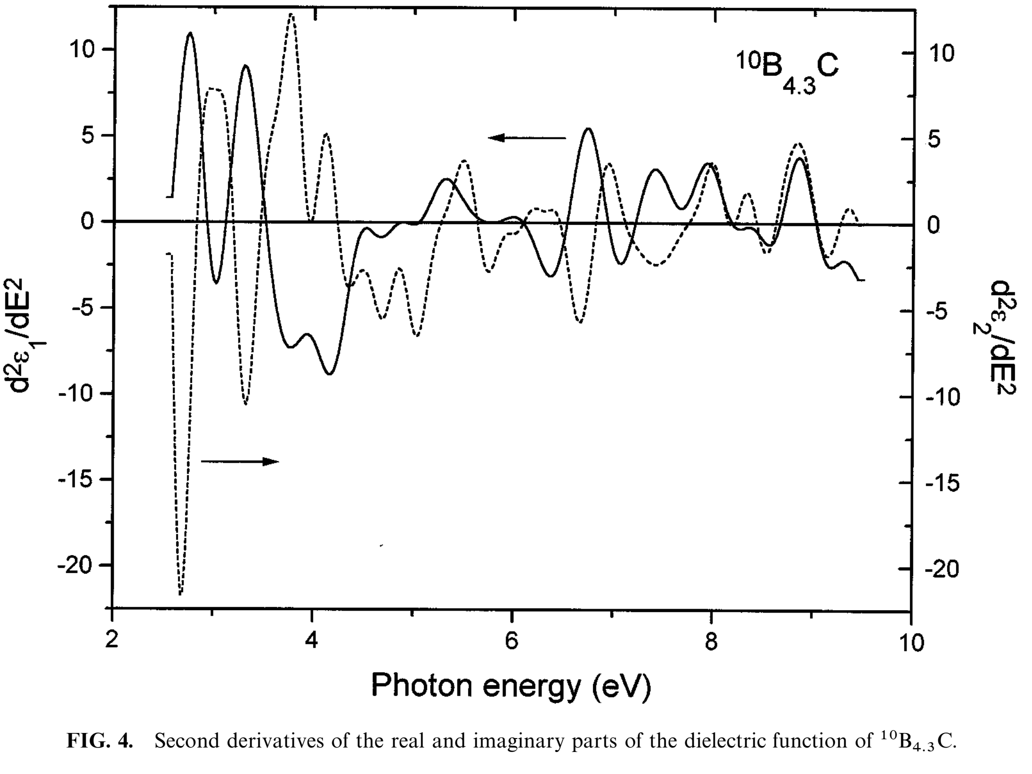

FIG. 4. Second derivatives of the real and imaginary parts of the dielectric function of $^{10}B_{4.3}C$.

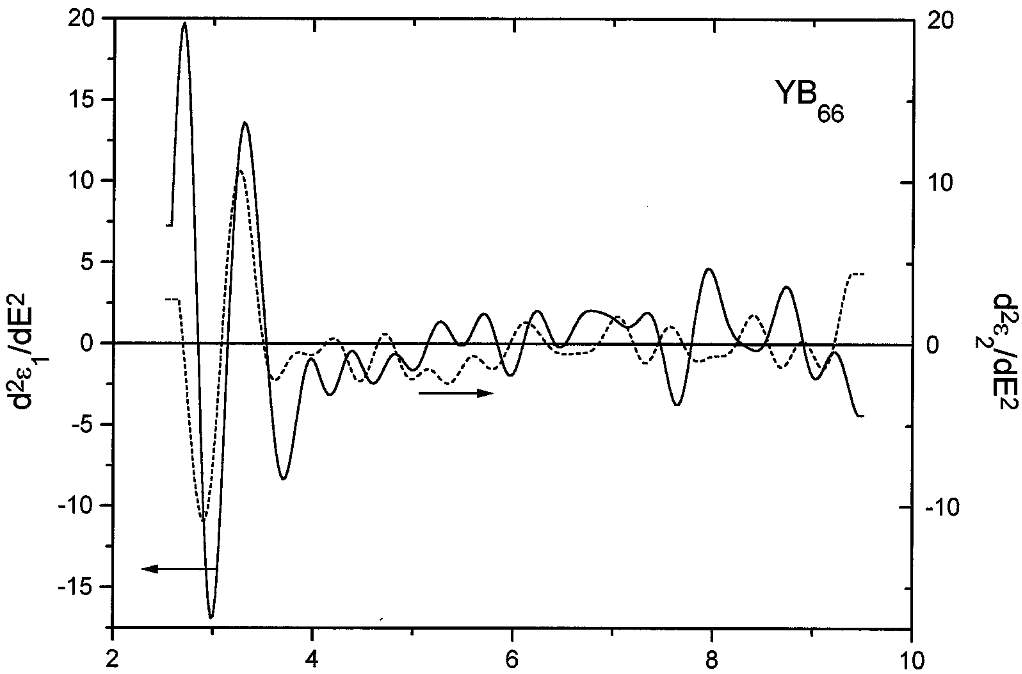

FIG. 5. Second derivatives of the real and imaginary parts of the dielectric function of YB_{66}.

agrees qualitatively with the close sequences of van Hove singularities experimentally found (Tables 1–3). The theoretically expected positions of those critical points, which are due to extrema of the energy bands, are the energetical distances of the calculated density of states maxima in valence and conduction band respectively. Attempts to correlate the energetical positions of the accordingly obtained maxima of the combined densities of states with the critical points derived from the dielectric function were only successful in the case of the B_{12} cluster calculation by Shirai and Nakamatsu (15) compared with the results obtained on β-rhombohedral boron (Fig. 6). Only few transitions remain unattributed. According to Shirai (21) his result depends only weakly on the individual crystal structure and in particular no considerable difference is expected between α-rhombohedral boron, for which the calculation was performed, and β-rhombohedral boron, for which the good correlation with the critical points has been established. Apart from those critical points, which are due to extrema in the energy band structures, there may be further ones evoked by nonhorizontal parallel courses of conduction and valence bands. These cannot be obtained from the calculated densities of states and may be the reason for the few nonattributable van Hove singularities in Fig. 6.

TABLE 1
β-Rhombohedral Boron, Minima of the Second Derivatives of ε_1 and ε_2

ε_1	ε_2	Type	ΔE_{crit} (estimated)
2.65	2.675		
3.0	3.325	M 1	3.15
3.625	4.0	M 1	3.8
4.45	4.525	M 1	4.5
5.35	5.525	?	5.4
6.025	6.2	M 1	6.1
6.475	6.65	M 1	6.6
	6.925		
7.6	7.4	M 3	7.5
8.075	8.075	M 2	8.1
8.55	8.5	M 3	8.53
8.975	8.925	M 3	8.95

Note. Type of critical points is estimated from the first derivative; critical point energies ΔE_{crit} are estimated according to the typical position relative to the second derivative minima.

Within the accuracy of measurement in the case of boron carbide the energetical positions of the van Hove singularities remain unchanged throughout the whole homogeneity range, while the values of the dielectric function change considerably. This is at least qualitatively consistent with the structure elements (B_{12} icosahedra, $B_{11}C$ icosahedra, C–B–C and C–B–B chains) varying only in concentration in the whole homogeneity range. Only the density of chainless unit cells is zero at the carbon-rich limit with the mostly homogeneous structure and increases with decreasing carbon content to about 50% close to the boron-rich limit (22). To check the correlation between dielectric function and structure, in Fig. 7 the values of ε_2 at different characteristic

TABLE 2
Boron Carbide, Minima of the Second Derivatives of ε_1 and ε_2 in eV

$B_{4.3}C$ (+C)		$^{10}B_{4.3}C$		$B_{4.23}C$		$B_{4.51}C$		$B_{4.66}C$		$B_{6.28}C$		$B_{6.4}C$		$B_{8.52}C$		$B_{10.37}C$		$^{10}B_{4.3}C$	
ε_1	ε_2	ε_1	ε_2	ε_1	ε_2	ε_1	ε_2	ε_1	ε_2	ε_1	ε_2	ε_1	ε_2	ε_1	ε_2	ε_1	ε_2	Type	ΔE_{crit}
	2.7		2.625		2.625						2.7				2.625		2.625	M1	
3.0	3.35	2.99	3.325	3.05	3.33	3.0	3.425	2.875	3.425	3.0	3.5	2.975	3.425	2.925	3.325	3.025	3.325	M1	3.2
3.75	4.0	3.8	3.975	3.75	4.025	3.725		3.725		3.725		3.9		3.75	3.975	3.7	4.075	M0	3.7
4.175	4.45	4.175	4.35	4.125	4.46	4.15	4.3	4.1	4.3	4.15			4.575	4.125	4.35	4.125	4.45	M1	4.3
4.55	4.775	4.65	4.68	4.675	4.9	4.525		4.525	4.825	4.675	4.825	4.8		4.625	5.0			M1	4.8
4.975	5.375	5.0	5.025	5.15	5.5	4.975	5.45	4.95	5.425		5.4		5.475	5.0	5.5		5.525	M1	5.0
5.675	5.775	5.625	5.75	5.625		5.45		5.6		5.375		5.525		5.5	5.725			M0	5.6
		5.875	6.0															M2(?)	5.9
6.275	6.65	6.375	6.675	6.4	6.475	6.0	6.475	6.25	6.45	6.25	6.425	6.325	6.525	6.2	6.725	6.4	6.5	M1	6.5
6.875	7.375	7.02	7.1	6.975	7.5	6.675		6.725		7.075			7.075	7.275	7.35	7.05	7.225	M1	7.1
		7.275	7.425															M1(?)	7.3
7.7	7.875	7.65	7.8	7.425	7.8	7.6	7.325	7.825	7.325	7.575	7.65	7.7		7.675	7.8	7.62	7.575	M2	7.9
	8.275	8.175	8.175	7.9		8.025				8.1			8.175	8.125	8.15	8.175	8.35	M1	8.2
8.525	8.675	8.45	8.525	8.525	8.625	8.575	8.525	8.325	8.525		8.575			8.575	8.675	8.7	8.75	M3	8.5
9.2		9.15	9.15	9.025		8.975		8.8		8.7		8.675	8.725	9.0		9.175		M0	9.1

Note. Type of critical points is estimated from the first derivative; energy of the critical points ΔE_{crit} is estimated according to the typical position relative to the second derivative minima.

photon energies are plotted versus the carbon content. While the values of the narrow peaks at lower energies increase roughly monotonously with decreasing carbon content, the values within the broad peak at higher energies follow approximately the concentration of B_{12} icosahedra. This underlines the importance of the icosahedra for the energy band structure. Only the slope of ε_2 at the intermediate energy 4.7 eV is ambiguous.

TABLE 3
YB_{66}, Minima of the Second Derivatives of ε_1 and ε_2

ε_1	ε_2	Type	ΔE_{crit} (estimated)
$\lesssim$2.575	2.675	M 2	2.7
2.95	2.95	M 0	2.9
3.425	3.625	M 0	3.4
3.75	4.025	M 1	3.9
M 1	4.45	M 1	4.3
4.625	4.95	M 1	4.8
5.0	5.3	M 1	5.2
5.525	5.85	M 1	5.7
6.0	6.5	M 0	5.9
6.375	6.725	M 1	6.6
7.275	7.325	M 0	7.2
7.6	7.825	M 1	7.7
7.825	8.175	M 1	8.0
8.4	8.7	M 1	8.5
8.975	9.1	M 0	9.2

Note. Type of critical points is estimated from the first derivative; critical point energies ΔE_{crit} estimated according to the typical position relative to the second derivative minima.

An essential point to be considered in the dielectric function is the effect of structure distortions, which are of different kind in the boron-rich solids. At first the isotope distribution in natural boron (19.8% ^{10}B, 80.2% ^{11}B) must be obeyed. Its effect on the dielectric function is obvious: For ^{10}B-enriched boron carbide, ε_2 exhibits much clearer maxima compared with natural boron carbide, of nearly the same composition (see Fig. 2). The reason is the considerably different zero point energy of the boron isotopes caused by the mass difference of about 10%. This leads to distortions of the icosahedra known from investigations of the IR and Raman active phonons (23) and correspondingly to energetically less-defined molecular orbitals of the icosahedra forming the energy bands in the solids.

The second kind of distortion is due to the substitution of carbon for boron atoms on sites in the icosahedra. However, it was shown in (24) that in boron carbide this distortion of the icosahedron is covered up by much stronger structure distortions caused by the composition-dependent structure variation, in particular by the chainless unit cells: The most homogeneous structure is found at the carbon-rich limit of the homogeneity range (19 at. % C); the strongest disorder exists at about 13.5 at.% C followed by a narrow range of higher order close to 11 at. % C and again a range of strong disorder toward the boron-rich limit of the homogeneity range. This tendency is clearly seen in the dielectric function, too, showing pronounced peaks of ε_2 for compositions with ordered structures and smeared peaks for compositions with disordered structures.

The values of the peaks at lower energies increase slightly with decreasing carbon content hence following roughly the concentration of chainless unit cells with strongly distorted

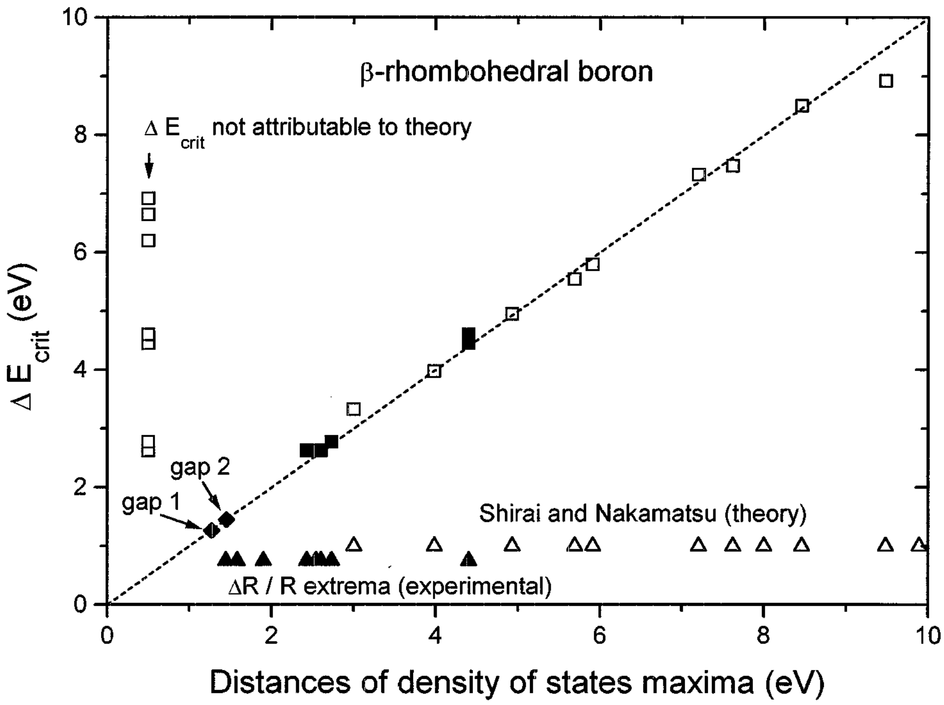

FIG. 6. Critical points ΔE_{crit} of β-rhombohedral boron attributed to the density of states calculation of the B_{12} cluster by Shirai and Nakamatsu (15) □, to $\Delta R/R$ extrema ■ (27). ◆ gaps derived from the absorption edge (3).

icosahedra (22). This seems to indicate that the combined density of states between 2.5 and 4 eV increases with increasing density of distorted icosahedra.

When these results are applied to YB_{66}, the pronounced structures in the dielectric function and the low combined density of states at lower energies lead to the conclusion that

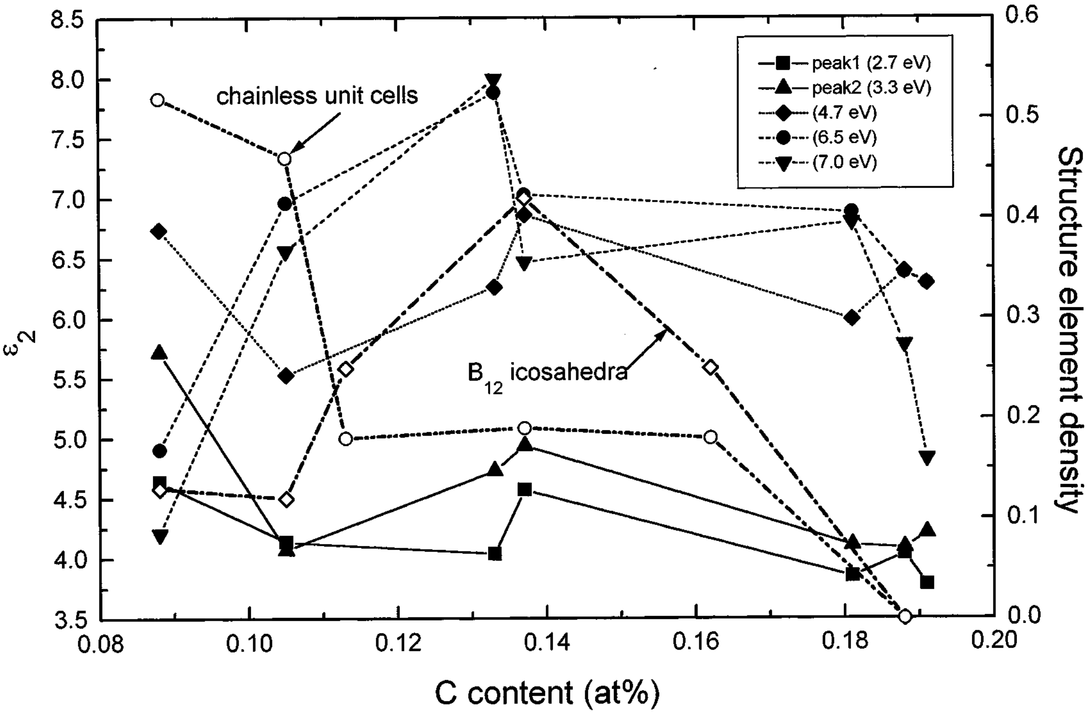

FIG. 7. Values of the imaginary part of the dielectric function ε_2 of boron carbide at characteristic energies versus carbon content. Density of B_{12} icosahedra and density of chainless unit cells (16) for comparison.

the crystal structure of YB_{66} (probably in particular the icosahedra) is only little distorted, and the energy band structure consists rather of a dense sequence of single orbitals originating of the large number of atoms and structure elements respectively per unit cell than of orbitals considerably broadened because of structural distortions. This supports the conclusion made in (7) that the electronic transport in YB_{66} is strongly influenced by trapping events and not by amorphous-like localized states, and yields a further argument against Golikova's amorphous concept (25, 26) that attributes to the boron-rich solids a continuous transition from the crystalline to the amorphous state depending on the number of atoms per unit cell.

ACKNOWLEDGMENTS

The authors are grateful to Dr. H. Kölker, Consortium für Elektrochemische Industrie (Wacker-Chemie), Munich, for providing the high-purity β-rhombohedral boron, to Dr. K. A. Schwetz, Elektroschmelzwerk Kempten, Dr. B. Krismer and Dr. D. Fister, H. C. Starck, Goslar and Laufenburg for providing the boron carbides, and to Dr. K. Shirai, Osaka, for a valuable discussion.

REFERENCES

1. R. Franz and H. Werheit, *Europhys. Lett.* **9,**145 (1989).
2. H. Werheit, Boron, *in* "Landolt-Börnstein Numerical Data and Functional Relationships in Science and Technology" (O. Madelung, M. Schulz, and H. Weiss, Eds.), New Series, Vol. 17e, p. 9. Springer, Berlin, 1983.
3. H. Werheit, M. Laux, and U. Kuhlmann, *Phys. Status Solidi B* **176,** 415 (1993).
4. H. Werheit, M. Laux, U. Kuhlmann, and R. Telle, *Phys. Status Solidi B* **K172,** 81 (1992).
5. G. A. Slack, T. F.McNelly, and E. A. Taft, *J. Phys. Chem. Solids* **44,** 249 (1983).
6. H. Werheit, U. Kuhlmann, K. Shirai, and Y. Kumashiro, *J. Alloys Compd.* **233,** 121 (1996).
7. U. Kuhlmann, H. Werheit, J. Hassdenteufel, and T. Tanaka, *in* "Proc. 11th Int. Symp. Boron, Borides and Related Comp, Tsukuba, 1993," JJAP Series 10, p. 82, (1994).
8. H. Werheit, U. Kuhlmann, G. Krach, I. Higashi, T. Lundström, and Y. Yu, *J. Alloys Compd.* **202,** 269 (1993).
9. H. Werheit, G. Krach, U. Kuhlmann, I. Higashi, V. N. Gurin, and M. M. Korsukova, *in* "Proc. 11th Int. Symp. Boron, Borides and Related Comp, Tsukuba, 1993," JJAP Series 10, p.96, 1994.
10. D. R. Armstrong, J. Bolland, and P. G. Perkins, *Theor. Chim. Acta* **64,** 501 (1984).
11. D. R. Armstrong, *in* "Proc. 9th Intern. Symp. Boron, Borides and Related Compounds, Duisburg" (H. Werheit, Ed.), p. 125. University of Duisburg, 1987.
12. L. Kleinman, *in* "AIP Conf. Proc. 231" (D. Emin, T. L. Aselage, A. C. Switendick, B. Morosin, and C. L. Beckel, Eds.), p. 13. Albuquerque, NM, 1990.
13. D. W. Bullett, *in* "Proc. 11th Int. Symp. Boron, Borides and Related Comp, Tsukuba, 1993," JJAP Series 10, p.31, 1994.
14. A. C. Switendick, *in* "The Physics and Chemistry of Carbides, Nitrides and Borides" (R. Freer, Ed.), p. 525. Kluwer, Dordrecht, 1990.
15. K. Shirai and H. Nakamatsu, *in* "Proc. 11th Int. Symp. Boron, Borides and Related Comp, Tsukuba, 1993," JJAP Series 10, p. 70, 1994.
16. U. Kuhlmann, H. Werheit, and K. A. Schwetz, *J. Alloys Compd.* **189,** 249 (1992).
17. T. Tanaka, Y. Ishizawa, J. Wong, Z. U. Rek, M. Rowen, F. Schäfers, and B. R. Müller, *in* "Proc. 11th Int. Symp. Boron, Borides and Related Comp, Tsukuba, 1993," JJAP Series 10, p. 110, 1994.
18. H. Binnenbruck, A. Hausen, P. Runow, and H. Werheit, *Z. Naturforsch. a* **25,** 1431 (1970).
19. R. L. Johnson, J. Barth, M. Cardona, D. Fuchs, and A. M. Bradshaw, *Nucl. Instrum. Methods A* **290,** 606 (1990).
20. G. Jungk, *Exp. Tech. Phys.* **23,** p. 356, (1975).
21. K. Shirai, personal communication (1996).
22. U. Kuhlmann, H. Werheit, and K. A. Schwetz, *J. Alloys Compd.* **189,** 249 (1992).
23. U. Kuhlmann, Thesis, Gerhard Mercator University Duisburg (1994).
24. H. Werheit, U. Kuhlmann, and T. Lundström, *J. Alloys Compd.* **204,** 197 (1994).
25. O. A. Golikova, *Phys. Status. Solidi A* **51,** 11 (1979).
26. O. A. Golikova, *in* "Proc. 9th Intern. Symp. Boron, Borides and Related Compounds, Duisburg" (H. Werheit, Ed.), p. 108, University of Duisburg, 1987.